

Bounds on the Capacity of Memoryless Simplified Fiber-Optical Channel Models

Kamran Keykhosravi, *Student Member, IEEE*,

Giuseppe Durisi, *Senior Member, IEEE*,

and Erik Agrell, *Senior Member, IEEE*.

Abstract

A number of simplified models have been proposed for the fiber-optical channel and have been extensively used in the literature. Although these models are mainly developed for the low-power regime, they are used at moderate or high powers as well. It remains unclear to what extent the capacity of these models is affected by the simplifying assumptions under which they are derived. In this paper, the capacity of three memoryless channel models, which are obtained applying different simplifying assumptions to the same physical fiber-optical channel, is investigated. First, the capacity of a memoryless model that is obtained through a perturbation method is bounded tightly and its capacity pre-log is proven to be 3. Second, a channel model based on the logarithmic perturbation method is considered. The capacity is proven to be $\log(1 + \text{SNR})$, where SNR is the signal-to-noise ratio. This implies that the capacity pre-log is one. Third, a memoryless nonlinear Schrödinger channel is studied. The capacity pre-log of this model is known to be $1/2$. We establish

This work was supported by the Swedish Research Council (VR) under Grant 2013-5271.

Part of this work has been accepted for presentation at the 43th European Conference on Optical Communication (ECOC 2017).

The authors are with the Department of Electrical Engineering, Chalmers University of Technology, Gothenburg 41296, Sweden (e-mail: kamrank@chalmers.se; durisi@chalmers.se; agrell@chalmers.se).

a novel upper bound that confines the capacity of this channel to a much narrower range than the previously known upper bound. Since all three models represent the same physical channel, the fact that each model yields a different capacity pre-log highlights that care must be exercised in using simplified channel models in the high-power regime.

Index Terms

Achievable rate, information theory, optical fiber, channel capacity, nonlinear channel.

I. INTRODUCTION

The vast majority of the global Internet traffic is conveyed through fiber-optical networks, which form the backbone of our information society. To cope with the growing data demand, the fiber-optical networks have evolved from regenerated direct-detection systems to coherent wavelength division multiplexing (WDM) systems [1]. Newly emerging bandwidth-hungry services, like internet-of-thing applications and cloud processing, require even higher data rates. Motivated by this ever-growing demand, an increasing attention has been devoted in recent years to the analysis of the capacity of the fiber-optical channel.

Finding the capacity of the fiber-optical channel that is governed by the generalized nonlinear Schrödinger (NLS) equation [2, Eq. (1)], which captures the effects of Kerr nonlinearity, chromatic dispersion, and amplification noise, remains an open problem. The information-theoretic analysis of the NLS channel is cumbersome because of a complicated signal–noise interaction caused by the interplay between the nonlinearity and the dispersion. Using the mismatch-decoding framework [3], a number of lower bounds on the capacity of this channel have been developed (see, for example, [4] and [5]). To establish an upper bound, Kramer *et al.* [6] used the split-step Fourier (SSF) method, which is a standard approach to solve the NLS equation numerically [7, Sec. 2.4.1], to derive a discrete-time channel model. They proved that the capacity of this discrete-time model is upper-bounded by that of an

equivalent AWGN channel. In contrast to the available lower bounds, which fall to zero or saturate at high powers, this upper bound, which is the only one available for a realistic fiber channel model, grows unboundedly.

Since the information-theoretic analysis of the NLS channel is difficult, to approximate capacity one can resort to simplified models, a number of which have been studied in the literature (see [8] and references therein for a recent review). Two approaches to obtain such models are to use the regular perturbation or the logarithmic perturbation methods. In the former, the effects of nonlinearity are captured by an additive perturbative term [9], [10]. This approach yields a discrete-time channel with input–output relation $\mathbf{y}_l = \mathbf{x}_l + \Delta\mathbf{x}_l + \mathbf{n}_l$ [8, Eq. (5)], where \mathbf{x}_l and \mathbf{y}_l are the transmitted and the received symbols, respectively; \mathbf{n}_l is the amplification noise; and $\Delta\mathbf{x}_l$ is the perturbative nonlinear distortion. This model holds under the simplifying assumption that both the nonlinearity and the signal–noise interaction are weak, which is reasonable at low power.

Regular perturbative fiber-optical channel models, with or without memory, have been extensively investigated in the literature. In [11], a first-order perturbative model for WDM systems with arbitrary filtering and sampling demodulation and coherent detection is proposed. Using this model, the authors of [11] show that the impairments in a single WDM channel are highly affected by the modulation used on the neighboring channels. In [12], the influence of four-wave-mixing interference on the capacity of a memoryless simplified perturbative WDM channel is studied for three different statistical models of the nonlinear crosstalk. The authors show that for different behavioral models the capacity may go to infinity or zero. The capacity of a perturbative multiple-access channel is studied in [13]. It is shown that the nonlinear crosstalk between channels does not affect the capacity region when the information from all the channels is optimally used at each detector. However, if joint processing is not possible, the channel capacity is limited by the inter channel distortion.

Another class of simplified models, which are equivalent to the regular perturbative

ones up to a first-order linearization, is that of logarithmic perturbative models, where the nonlinear distortion term $\Delta \mathbf{x}_l$ is modeled as a phase shift. This yields a discrete-time channel with input–output relation $\mathbf{y}_l = \mathbf{x}_l e^{j\Delta \mathbf{x}_l} + \mathbf{n}_l$ [8, Eq. (7)]. In [14] and [15], a memoryless logarithmic perturbative optical channel for a two-user WDM transmission system is developed and its capacity region is studied in the high-power regime. It is shown that the capacity pre-log pair (1,1) is achievable, where the capacity pre-log is defined as the asymptotic limit of $\mathcal{C}/\log P$ for $P \rightarrow \infty$, where P is the input power and \mathcal{C} is the capacity.

Despite the fact that the aforementioned simplified channels are valid in the low-power regime, these models are often used also in the moderate- and high-power regimes. Currently, it is unclear to what extent the simplifications used to obtain these models influence the capacity at high powers. To find out, we study the capacity of two memoryless perturbative models, namely, a *regular perturbative channel (RPC)*, and a *logarithmic perturbative channel (LPC)*. To assess accuracy of these two perturbative models, we investigate also the capacity of the *memoryless NLS channel (MNC)*, which is obtained from the zero-dispersion NLS equation without further approximations, and whose capacity serves as benchmark. A number of results are available on the capacity of this channel model. In [16], a lower bound on the per-sample capacity of the memoryless NLS channel is derived, which proves that the capacity goes to infinity with power. In [17], the capacity of the same channel is evaluated numerically. Furthermore, it is shown that the capacity pre-log is 1/2. The only known nonasymptotic upper bound on the capacity of this channel is $\log(1 + \text{SNR})$ (bits per channel use) [6], where SNR is the signal-to-noise ratio. This upper bound holds also for the general case of nonzero dispersion.

The novel contributions of this paper are as follows: First, we tightly bound the capacity of the RPC model and prove that its capacity pre-log is 3. Second, the capacity of the LPC is readily shown to be the same as that of an AWGN channel with the same input and noise power. Hence, the capacity pre-log of the LPC is 1. Third, we establish a novel upper bound

[18] on the capacity of the MNC. Our upper bound improves the previously known upper bound [6] on the capacity of this channel significantly and together with the available lower bounds allows one to characterize the capacity of the MNC accurately.

Although all three models represent the same physical optical channel, their capacities behave very differently in the high-power regime. This result highlights the profound impact of the simplifying assumptions on the capacity at high powers, and indicates that care should be taken in translating the results obtained based on these models into guidelines for system design.

The rest of this paper is organized as follows. In Section II, we introduce the three channel models. In Section III, we present upper and lower bounds on the capacity of these channels and establish the capacity pre-log of the perturbative models. Numerical results are provided in Section IV. We conclude the paper in Section V. The proofs of all theorems are given in the appendices.

Notation: Random quantities are denoted by boldface letters. We use $\mathcal{CN}(0, \sigma^2)$ to denote the complex zero-mean circularly symmetric Gaussian distribution with variance σ^2 . We write $\mathcal{R}(x)$, $|x|$, and $\angle x$ to denote the real part, the absolute value, and the phase of a complex number x . All logarithms are in base two. The mutual information between two random variables \mathbf{x} and \mathbf{y} is denoted by $I(\mathbf{x}; \mathbf{y})$. The entropy and differential entropy are denoted by $H(\cdot)$ and $h(\cdot)$, respectively. Finally, we use $\mathbf{1}(\cdot)$ for the indicator function.

II. CHANNEL MODEL

The fiber-optical channel is well-modeled by the NLS equation, which describes the propagation of a complex baseband electromagnetic field through a lossy single-mode fiber as

$$\frac{\partial \mathbf{a}}{\partial z} + \frac{\alpha - g}{2} \mathbf{a} + j \frac{\beta_2}{2} \frac{\partial^2 \mathbf{a}}{\partial t^2} - j \gamma |\mathbf{a}|^2 \mathbf{a} = \mathbf{n}. \quad (1)$$

Here, $\mathbf{a} = \mathbf{a}(t, z)$ is the complex baseband signal at time t and location z . The parameter γ is the nonlinear coefficient, β_2 is the group-velocity dispersion parameter, α is the attenuation

constant, $g = g(z)$ is the gain profile of the amplifier, and $\mathbf{n} = \mathbf{n}(t, z)$ is the white Gaussian amplification noise. The third term on the left-hand side of (1) is responsible for the channel memory and the fourth term for the channel nonlinearity.

To compensate for the fiber losses, two types of signal amplification can be deployed, namely, distributed and lumped amplification. The former method compensates the fiber loss continuously along the fiber, whereas the latter method boosts the signal power by dividing the fiber into several spans and using an optical amplifier at the end of each span. With distributed amplification, which we focus on in this paper, the noise can be described by the autocorrelation function

$$\mathbf{E}[\mathbf{n}(z, t)\mathbf{n}^*(z', t')] = \alpha n_{\text{sp}} h \nu \delta_{W_N}(t - t') \delta(z - z'). \quad (2)$$

Here, n_{sp} is the spontaneous emission factor, h is Planck's constant, and ν is the optical carrier frequency. Also, $\delta(\cdot)$ is the Dirac delta function and $\delta_{W_N}(x) = W_N \text{sinc}(W_N x)$, where W_N is the noise bandwidth. In this paper, we shall focus on the ideal distributed-amplification case $g(z) = \alpha$.

Next, two perturbative channel models are introduced to approximate the solution of the NLS equation (1). Both of these models have been used extensively in the literature to describe the fiber-optical link under some simplifying assumptions. We shall focus on the nondispersive case $\beta_2 = 0$.

Regular perturbative channel (RPC) : In the regular perturbation method, the output of the NLS channel (1) is approximated as [8, Eq. (5)]

$$\mathbf{a}(z, t) = \mathbf{a}^L(z, t) + \Delta \mathbf{a}(z, t) + \mathbf{n}(z, t) \quad (3)$$

where $\mathbf{a}^L(z, t)$ is the solution of the NLS equation for $\gamma = 0$, $\Delta \mathbf{a}(z, t)$ is the nonlinear perturbation term, and $\mathbf{n}(z, t)$ is the amplification noise. One approach to compute $\Delta \mathbf{a}(z, t)$

is to write the solution of the NLS equation as a power series expansion of γ , i.e.,

$$\mathbf{a}(z, t) = \sum_{i=0}^{\infty} \mathbf{a}_i(z, t) \gamma^i \quad (4)$$

where the signals $\mathbf{a}_i(z, t)$ can be determined by substituting (4) into (1) [19], [20]. Proceeding as in [20, Sec. 3] and setting $\beta_2 = 0$ (zero-dispersion assumption), one obtains $\mathbf{a}_0(z, t) = \mathbf{a}(0, t)$ and $\mathbf{a}_1(z, t) = jL|\mathbf{a}(0, t)|^2\mathbf{a}(0, t)$, where L is the fiber length. By keeping only the first two terms in the infinite sum in (4) and sampling the signal at the receiver at the symbol rate, we derive the discrete-time memoryless channel

$$\mathbf{y} = \mathbf{x} + j\eta|\mathbf{x}|^2\mathbf{x} + \mathbf{n}. \quad (5)$$

Here, $\mathbf{n} \sim \mathcal{CN}(0, P_N)$,

$$P_N = 2\alpha n_{\text{sp}} h\nu L W_N \quad (6)$$

is the total noise power, and

$$\eta = \gamma L. \quad (7)$$

We refer to (5) as the RPC.

Logarithmic perturbative channel (LPC): Another method for approximating the solution of the NLS equation (1) is to use logarithmic perturbation, where the output signal is written as

$$\mathbf{a}(z, t) = \mathbf{a}(0, t) \exp\left(j \sum_{i=1}^{\infty} \gamma^i \mathbf{a}_i^{\text{lp}}(z, t)\right) + \mathbf{n}(z, t). \quad (8)$$

Here, the signals $\mathbf{a}_i^{\text{lp}}(z, t)$ can be determined by substituting (8) in the NLS equation (1). By setting $\beta_2 = 0$ and by using [21, Eq. 10b], one obtains $\mathbf{a}_1^{\text{lp}}(z, t) = jL|\mathbf{a}(0, t)|^2$. Keeping only the first term in the infinite sum in (8) and sampling the output signal at the receiver, we obtain the discrete-time memoryless channel

$$\mathbf{y} = \mathbf{x} e^{j\eta|\mathbf{x}|^2} + \mathbf{n} \quad (9)$$

where $\mathbf{n} \sim \mathcal{CN}(0, P_N)$, P_N is defined in (6), and η is defined in (7). We note that channels (5) and (9) are equal up to a first-order linearization.

Memoryless NLS Channel (MNC): To assess the accuracy of the simplified channels (5) and (9), we shall also study the underlying NLS channel in (1) for the case $\beta_2 = 0$. Let \mathbf{r}_0 and θ_0 be the amplitude and the phase of a transmitted symbol \mathbf{x} and \mathbf{r} and θ be those of the received samples \mathbf{y} . When dispersion is ignored, the discrete-time channel input–output relation can be described by the conditional probability density function (pdf) [22, Ch. 5]

$$f_{\mathbf{r},\theta|\mathbf{r}_0,\theta_0}(r, \theta|r_0, \theta_0) = \frac{f_{\mathbf{r}|\mathbf{r}_0}(r | r_0)}{2\pi} + \frac{1}{\pi} \sum_{m=1}^{\infty} \mathcal{R}(C_m(r)e^{jm(\theta-\theta_0)}). \quad (10)$$

The conditional pdf $f_{\mathbf{r}|\mathbf{r}_0}(r | r_0)$ and the Fourier coefficients $C_m(r)$ in (10) are given by

$$f_{\mathbf{r}|\mathbf{r}_0}(r | r_0) = \frac{2r}{P_N} \exp\left(-\frac{r^2 + r_0^2}{P_N}\right) I_0\left(\frac{2rr_0}{P_N}\right) \quad (11)$$

$$C_m(r) = \frac{r \sec(x_m)}{s_m} \exp\left(\frac{r_0^2 x_m \tan(x_m)}{P_N} - \frac{r^2 + \alpha_m^2}{2s_m}\right) I_m\left(\frac{\alpha_m r}{s_m}\right). \quad (12)$$

Here, $I_m(\cdot)$ denotes the m th order modified Bessel function of the first kind. Also, we have

$$x_m = \left(\frac{2jm\gamma r_0^2 P_N L}{2r_0^2 + P_N}\right)^{1/2} \quad (13)$$

$$\alpha_m = r_0 \sec(x_m) \quad (14)$$

$$s_m = \frac{P_N \tan(x_m)}{2x_m}. \quad (15)$$

In the next section, we study the capacity of the channel models given in (5), (9), and (10). Since all of these models are memoryless, their capacities under a power constraint P is given by

$$\mathcal{C} = \sup I(\mathbf{y}, \mathbf{x}) \quad (16)$$

where the supremum is over all probability distributions of \mathbf{x} that satisfy the average-power constraint

$$\mathbb{E}[|\mathbf{x}|^2] \leq P. \quad (17)$$

III. ANALYTICAL RESULTS

In this section, we study the capacity of the RPC, the LPC, and the MNC models. All these models represent the same fiber-optical channel and share the same set of parameters. Bounds on the capacity of the RPC in (5) are provided in Theorems 1–3. Specifically, in Theorem 1 we establish a closed-form lower bound, which, together with the upper bound provided in Theorem 2, tightly bounds capacity (see Section IV). A different upper bound is provided in Theorem 3. Numerical evidence suggests that this alternative bound is less tight than the one provided in Theorem 2 (see Section IV). However, this alternative bound has a simple analytical form, which makes it easier to characterize it asymptotically. By using the bounds derived in Theorem 1 and Theorem 3, we prove that the capacity pre-log of the RPC is 3. In Theorem 4, we present for completeness the (rather trivial) observation that the capacity of the LPC in (9) coincides with that of an equivalent AWGN channel. Hence, the capacity pre-log is 1. Finally, in Theorem 5, we provide an upper bound on the capacity of the MNC in (10), which improves the previous known upper bound [6] significantly, and, together with the available capacity lower bounds, yields a tight characterization of capacity (see Section IV).

A. Capacity Analysis of the RPC

Theorem 1. The capacity \mathcal{C}_{RPC} of the RPC in (5) is lower-bounded by

$$\mathcal{C}_{\text{RPC}} \geq \text{L}_{\text{RPC}}(P) = \max_{\lambda} \left\{ \log \left(\frac{\lambda^2 + 6\eta^2}{\lambda^3 P_N} e^{\frac{12\eta^2}{\lambda^2 + 6\eta^2}} + 1 \right) \right\} \quad (18)$$

where λ is positive and satisfies the constraint

$$\frac{18\eta^2 + \lambda^2}{\lambda(6\eta^2 + \lambda^2)} \leq P. \quad (19)$$

Furthermore, the maximum in (18) is achieved by the unique real solution of the equation

$$P\lambda^3 - \lambda^2 + 6P\eta^2\lambda - 18\eta^2 = 0. \quad (20)$$

Proof: See Appendix I. ■

Theorem 2. The capacity of the RPC in (5) is upper-bounded by

$$\begin{aligned} \mathcal{C}_{\text{RPC}} &\leq U_{\text{RPC}}(P) \\ &= \min_{\mu>0, \lambda>0} \left\{ \log \frac{\mu^2 + 6\eta^2}{\mu^3 e P_N} + \lambda + \max_{s>0} \left\{ \mu \mathbb{E} \left[q(|\mathbf{y}|^2) \mid |\mathbf{x}|^2 = s \right] \log e - \lambda \frac{s + P_N}{P + P_N} \right\} \right\}. \end{aligned} \quad (21)$$

Here, $q(x) = g^{-1}(x)$, where $g(x) = x + \eta^2 x^3$.

Proof: See Appendix II. ■

Note that, given $|\mathbf{x}|^2 = s$, the random variable $|\mathbf{y}|^2/P_N$ is conditionally distributed as a noncentral chi-squared random variable with 2 degrees of freedom and noncentrality parameter $(s + \eta^2 s^3)/P_N$. This enables numerical computation of $U_{\text{RPC}}(P)$.

Theorem 3. The capacity of the RPC in (5) is upper-bounded by

$$\mathcal{C}_{\text{RPC}} \leq \tilde{U}_{\text{RPC}}(P) = \min_{\mu>0} \left\{ \log \left(\frac{\mu^2 + 6\eta^2}{\mu^3 e P_N} \right) + \mu(P + B) \log e \right\} \quad (22)$$

where

$$B = P_N + \frac{\sqrt{\pi P_N}}{12^{3/8} \sqrt{(\sqrt{3} - 1)\eta}}. \quad (23)$$

Furthermore, the minimum in (22) is achieved by the unique real solution of the equation

$$(P + B) \mu^3 - \mu^2 + 6\eta^2(P + B) \mu - 18\eta^2 = 0. \quad (24)$$

Proof: See Appendix III. ■

Pre-log analysis: By substituting $\mu = 1/P$ into (22), we see that

$$\lim_{P \rightarrow \infty} [\mathcal{C}_{\text{RPC}} - 3 \log(P)] \leq \log \left(\frac{6\eta^2}{P_N} \right). \quad (25)$$

Furthermore, since

$$\frac{18\eta^2 + \lambda^2}{\lambda(6\eta^2 + \lambda^2)} \leq \frac{18\eta^2 + 3\lambda^2}{\lambda(6\eta^2 + \lambda^2)} \quad (26)$$

$$= \frac{3}{\lambda} \quad (27)$$

we can obtain a valid lower bound on \mathcal{C}_{RPC} by substituting $\lambda = 3/P$ into (18). Doing so, we obtain

$$\lim_{P \rightarrow \infty} [\mathcal{C}_{\text{RPC}} - 3 \log(P)] \geq \log\left(\frac{2\eta^2 e^2}{9P_N}\right). \quad (28)$$

It follows from (25) and (28) that the capacity pre-log of the RPC is 3.

B. Capacity Analysis of the LPC

Theorem 4. The capacity of the LPC in (9) is

$$\mathcal{C}_{\text{LPC}} = \log\left(1 + \frac{P}{P_N}\right). \quad (29)$$

Proof: We use the maximum differential entropy lemma [23, Sec. 2.2] to upper-bound \mathcal{C}_{LPC} by $\log(1 + P/P_N)$. Then, we note that we can achieve this upper bound by choosing $\mathbf{x} \sim \mathcal{CN}(0, P)$. ■

C. Capacity Analysis of the MNC

A novel upper bound on the capacity of the MNC in (10) is presented in the following theorem [18].

Theorem 5. The capacity of the MNC in (10) is upper-bounded by

$$\mathcal{C}_{\text{MNC}} \leq U_{\text{MNC}}(P) \quad (30)$$

$$= \min_{\lambda > 0, \alpha > 0} \left\{ \alpha \log\left(\frac{P + P_N}{\alpha}\right) + \log(\pi\Gamma(\alpha)) + \lambda + \max_{r_0 > 0} \{g_{\lambda, \alpha}(r_0, P)\} \right\} \quad (31)$$

where $\Gamma(\cdot)$ denotes the Gamma function and

$$g_{\lambda, \alpha}(r_0, P) = (\alpha \log e - \lambda) \frac{r_0^2 + P_N}{P + P_N} + (1 - 2\alpha) \mathbb{E}[\log(\mathbf{r}) \mid \mathbf{r}_0 = r_0] \\ - h(\mathbf{r} \mid \mathbf{r}_0 = r_0) - h(\boldsymbol{\theta} \mid \mathbf{r}, \mathbf{r}_0 = r_0, \boldsymbol{\theta}_0 = 0). \quad (32)$$

TABLE I: Channel parameters.

Parameter	Symbol	Value
Attenuation	α	0.2 dB/km
Nonlinearity	γ	$1.27 \text{ (W} \cdot \text{km)}^{-1}$
Fiber length	L	5000 km
Noise bandwidth	W_N	32 GHz
Emission factor	n_{sp}	1
Photon energy	$h\nu$	$1.28 \cdot 10^{-19} \text{ J}$
Noise variance	P_N	-27.2 dBm

The upper bound $U_{\text{MNC}}(P)$ can be calculated numerically using the expression for the conditional pdf $f_{\mathbf{r}, \theta | r_0, \theta_0}(r, \theta | r_0, \theta_0)$ given in (10).

Proof: See Appendix IV. ■

IV. NUMERICAL EXAMPLES

We evaluate the bounds derived in Section III for a fiber-optical channel whose parameters are listed in Table I. Using (7), we obtain $\eta = 6350 \text{ W}^{-1}$.

Fig. 1 depicts the upper and lower bounds on the capacity of the RPC in (5) and the MNC in (10). The capacity (29) of the LPC in (9), which is equal to that of an equivalent AWGN channel, is plotted as well.

As can be seen from Fig. 1, the capacity of the RPC is tightly bounded between the upper bound $U_{\text{RPC}}(P)$ in (21) and the lower bound $L_{\text{RPC}}(P)$ in (18). The maximum relative gap between these two bounds is 0.8% (it occurs at -16 dBm). Furthermore, one can observe that although the alternative upper bound $\tilde{U}_{\text{RPC}}(P)$ in (22) is loose at low powers, it becomes

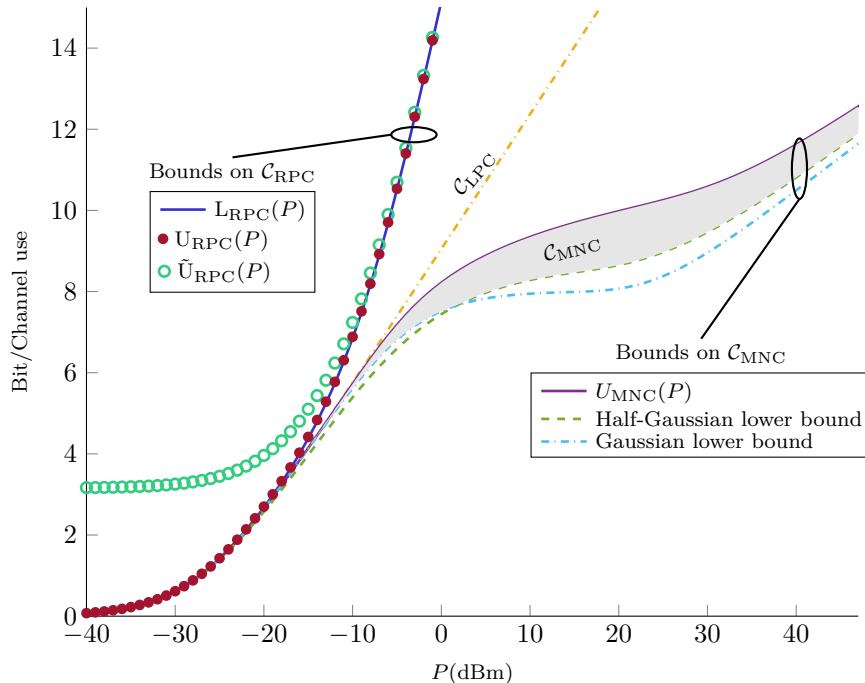


Fig. 1: Capacity bounds for the RPC in (5) and the MNC in (10), together with the capacity of the LPC in (9).

tight in the moderate- and high-power regimes. The relative gap between this upper bound and $L_{\text{RPC}}(P)$ is less than 0.5% at $P = 0$ dBm and this gap becomes smaller at higher powers.

We also plot the upper bound $U_{\text{MNC}}(P)$ on the capacity of the MNC together with two capacity lower bounds. It can be seen that $U_{\text{MNC}}(P)$ improves substantially on the upper bound given in [6], i.e., the capacity of the corresponding AWGN channel (29) (which coincides with \mathcal{C}_{LPC}). The two lower bounds are evaluated by calculating numerically the mutual information in (16) for a fixed input distribution. The first lower bound is obtained by considering a circularly-symmetric input distribution with half-Gaussian amplitude \mathbf{r}_0

$$f_{\mathbf{r}_0}(r_0) = \frac{\sqrt{2}}{\pi P} \exp\left(-\frac{r_0^2}{2P}\right). \quad (33)$$

It has been shown in [17] that (33) is capacity-achieving in the high-power regime. The second lower bound is based on a circularly-symmetric Gaussian input distribution, which achieves capacity whenever the nonlinearity is negligible, i.e., in the low-power regime. As

is evident from Fig. 1, in the high-power regime, the half-Gaussian lower bound is tighter than the Gaussian lower bound, while in the low-power regime the latter provides a tighter bound.

Fig. 1 suggests that \mathcal{C}_{MNC} experiences changes in slope at about 0 and 30 dBm. This can be explained as follows. Because of the nonlinearity, the signal experiences a phase shift that is a nonlinear function of the signal and the noise. In the moderate-power regime, the noise variance increases rapidly with the signal power, which reduces the information rate that can be transmitted through the signal phase. In the high-power regime, the phase of the received samples converges to a uniform distribution over the interval $[0, 2\pi)$ and essentially becomes independent of the transmitted signal. Hence, the information rate that can be transmitted through the signal phase is a unimodal function of the power that vanishes in the high-power regime, which explains the changes in the slope of \mathcal{C}_{MNC} .

As a final observation, we note that \mathcal{C}_{RPC} diverges from \mathcal{C}_{MNC} at about -15 dBm, whereas \mathcal{C}_{LPC} diverges from \mathcal{C}_{MNC} at about -5 dBm. Since the MNC describes the nondispersive NLS channel without any simplifying assumptions, this result shows that the perturbative models are grossly inaccurate in the high-power regime.

V. DISCUSSION AND CONCLUSION

The capacity of three memoryless optical channel models, namely, the RPC, the LPC, and the MNC were investigated. Two of these models, i.e., the RPC and the LPC, are based on perturbation theory and ignore signal–noise interaction, which makes them accurate only in the low-power regime. The third model, i.e., the MNC, describes accurately a memoryless fiber-optical channel governed by the NLS equation. By tightly bounding the capacity of the RPC, by characterizing the capacity of the LPC, and by developing a tight upper bound on the capacity of the MNC, we characterized the impact of the simplifying assumptions used to derive the RPC and the LPC on capacity. Our results indicate that the capacity of the

perturbative channels (i.e., the RPC and the LPC) is significantly different from that of the MNC at moderate and high powers. Specifically, the capacity pre-log is proved to be 3 for the RPC and 1 for the LPC, whereas the capacity pre-log of the MNC is 1/2. This result shows that the two perturbative models are grossly inaccurate at high powers.

APPENDIX I

PROOF OF THEOREM 1

The capacity of the regular perturbative channel can be written as

$$\mathcal{C}_{\text{RPC}} = \sup I(\mathbf{x}; \mathbf{y}) \quad (34)$$

where the supremum is over all the probability distributions on \mathbf{x} that satisfy the power constraint (17). Let

$$\mathbf{w} = \mathbf{x} + j\eta|\mathbf{x}|^2\mathbf{x}. \quad (35)$$

We have that

$$I(\mathbf{x}; \mathbf{y}) = h(\mathbf{y}) - h(\mathbf{y} | \mathbf{x}) \quad (36)$$

$$= h(\mathbf{w} + \mathbf{n}) - h(\mathbf{w} + \mathbf{n} | \mathbf{x}) \quad (37)$$

$$= h(\mathbf{w} + \mathbf{n}) - h(\mathbf{n}). \quad (38)$$

Using the entropy power inequality [23, Sec. 2.2] and the Gaussian entropy formula [24, Th. 8.4.1], we conclude that

$$h(\mathbf{w} + \mathbf{n}) \geq \log\left(2^{h(\mathbf{w})} + 2^{h(\mathbf{n})}\right) \quad (39)$$

$$= \log\left(2^{h(\mathbf{w})} + \pi e P_N\right). \quad (40)$$

Substituting (40) into (38), and using again the Gaussian entropy formula [24, Th. 8.4.1], we obtain

$$I(\mathbf{x}; \mathbf{y}) \geq \log\left(2^{h(\mathbf{w})} + \pi e P_N\right) - \log(\pi e P_N). \quad (41)$$

We take \mathbf{x} circularly symmetric. It follows from (35) that \mathbf{w} is also circularly symmetric. Using [25, Eq. (320)] to compute $h(\mathbf{w})$, we obtain

$$h(\mathbf{w}) = h(|\mathbf{w}|^2) + \log \pi. \quad (42)$$

Substituting (42) into (41), we get

$$I(\mathbf{x}; \mathbf{y}) \geq \log \left(\frac{2^{h(|\mathbf{w}|^2)}}{eP_N} + 1 \right). \quad (43)$$

Next to evaluate the right-hand side (RHS) of (43), we choose the following distribution for the amplitude square $\mathbf{s} = |\mathbf{x}|^2$ of \mathbf{x} :

$$f_{\mathbf{s}}(s) = \zeta (3\eta^2 s^2 + 1) e^{-\lambda s}, \quad s \geq 0. \quad (44)$$

The parameters $\lambda > 0$ and $\zeta > 0$ are chosen so that (44) is a pdf and so that the power constraint (17) is satisfied. We prove in Appendix I-A that by choosing these two parameters so that

$$\zeta = \frac{\lambda^3}{\lambda^2 + 6\eta^2} \quad (45)$$

and so that (20) holds, both constraints are met. In Appendix I-B, we then prove that

$$h(|\mathbf{w}|^2) = -\log \zeta + \zeta \left(\frac{1}{\lambda} + \frac{18\eta^2}{\lambda^3} \right) \log e. \quad (46)$$

Substituting (46) and (45) into (43), we obtain (18). Although not necessary for the proof, in Appendix I-C, we justify the choice of the pdf in (44) by showing that it maximizes $h(\mathbf{w})$.

A. Choosing ζ and λ

We choose the coefficients ζ and λ so that (44) is a valid pdf and $\mathbb{E}[\mathbf{s}] \leq P$. Note that

$$\int_0^{\infty} f_{\mathbf{s}}(s) ds = \int_0^{\infty} \zeta (3\eta^2 s^2 + 1) e^{-\lambda s} ds \quad (47)$$

$$= \zeta \frac{\lambda^2 + 6\eta^2}{\lambda^3}. \quad (48)$$

Therefore, choosing ζ according to (45) guarantees that $f_{\mathbf{s}}(s)$ integrates to 1. We next compute $E[\mathbf{s}]$:

$$E[\mathbf{s}] = \int_0^{\infty} s f_{\mathbf{s}}(s) ds \quad (49)$$

$$= \int_0^{\infty} s \zeta (3\eta^2 s^2 + 1) e^{-\lambda s} ds \quad (50)$$

$$= \zeta \left(\frac{18\eta^2}{\lambda^4} + \frac{1}{\lambda^2} \right). \quad (51)$$

Substituting (45) into (51), we obtain

$$E[s] = \frac{18\eta^2 + \lambda^2}{\lambda(\lambda^2 + 6\eta^2)}. \quad (52)$$

We see now that imposing $E[s] \leq P$ is equivalent to (19). Observe that the RHS of (52) and the objective function on the RHS of (18) are decreasing functions of λ . Therefore, setting the RHS of (52) equal to P , which yields (20), maximizes the objective function in (18).

Finally, we prove that (20) has a single positive root. We have

$$f(\lambda) = P\lambda^3 - \lambda^2 + 6P\eta^2\lambda - 18\eta^2 \quad (53)$$

$$= (\lambda^2 + 6\eta^2)(P\lambda - 1) - 12\eta^2. \quad (54)$$

Note that $f(\lambda) \rightarrow \infty$ as $\lambda \rightarrow \infty$ and that the RHS of (54) is negative when $\lambda < 1/P$. Furthermore, $f(\lambda)$ is monotonically increasing in the interval $[1/P, \infty)$. Indeed, when $\lambda \geq 1/P$,

$$\frac{d}{d\lambda} f(\lambda) = 3P\lambda^2 - 2\lambda + 6P\eta^2 \quad (55)$$

$$\geq 3\lambda - 2\lambda + 6P\eta^2 \quad (56)$$

$$> 0. \quad (57)$$

This yields the desired result.

B. Proof of (46)

To compute the differential entropy of $\mathbf{t} = |\mathbf{w}|^2$, we first determine the pdf of \mathbf{t} . By definition,

$$\mathbf{t} = \mathbf{s} + \eta^2 \mathbf{s}^3. \quad (58)$$

Let now $g(x) = x + \eta^2 x^3$. Since

$$\frac{d}{dx}g(x) = 1 + 3\eta^2 x^2 \quad (59)$$

we conclude that $g(x)$ is monotonically increasing for $x \geq 0$. Hence, $g(x)$ is one-to-one when $x \geq 0$ and its inverse

$$q(x) = g^{-1}(x) \quad (60)$$

is well defined. Thus, the pdf of \mathbf{t} is given by [26, Ch. 5]

$$f_{\mathbf{t}}(t) = \frac{f_{\mathbf{s}}(q(t))}{g'(q(t))} \quad (61)$$

$$= \frac{\zeta(3\eta^2 q^2(t) + 1) e^{-\lambda q(t)}}{3\eta^2 q^2(t) + 1} \quad (62)$$

$$= \zeta e^{-\lambda q(t)}, \quad t \geq 0. \quad (63)$$

Here, (62) holds because of (44). Using (63), we can now compute $h(\mathbf{t})$ as

$$h(\mathbf{t}) = - \int_0^{\infty} f_{\mathbf{t}}(t) \log(f_{\mathbf{t}}(t)) dt \quad (64)$$

$$= -\log \zeta + \lambda \zeta (\log e) \int_0^{\infty} q(t) e^{-\lambda q(t)} dt \quad (65)$$

$$= -\log \zeta + \lambda \zeta (\log e) \int_0^{\infty} r e^{-\lambda r} (1 + 3\eta^2 r^2) dr \quad (66)$$

$$= -\log \zeta + \lambda \zeta \left(\frac{1}{\lambda^2} + \frac{18\eta^2}{\lambda^4} \right) \log e \quad (67)$$

where in (66) we used the change of variables $r = q(t)$. This proves (46).

C. $f_{\mathbf{s}}(s)$ maximizes $h(\mathbf{w})$

We shall prove that the pdf $f_{\mathbf{s}}(s) = \zeta (3\eta^2 s^2 + 1) e^{-\lambda s}$, $s \geq 0$, maximizes $h(\mathbf{w})$. It follows from (42) that to maximize $h(\mathbf{w})$, we need to maximize $h(\mathbf{t})$. We assume that the power constraint is fulfilled with equality, i.e., that

$$\mathbb{E}[\mathbf{s}] = \int_0^\infty s f_{\mathbf{s}}(s) ds = P. \quad (68)$$

Using the change of variables $s = q(t)$, where $q(t)$ was defined in (60), we obtain

$$\int_0^\infty q(t) f_{\mathbf{s}}(q(t)) q'(t) dt = P. \quad (69)$$

Substituting (61) into (69) and using that $q'(t) = 1/g'(q(t))$, we obtain

$$\int_0^\infty q(t) f_{\mathbf{t}}(t) dt = P. \quad (70)$$

It follows now from [24, Th. 12.1.1] that the pdf that maximizes $h(\mathbf{t})$ is of the form $f_{\mathbf{t}}(t) = e^{\lambda_0 + \lambda_1 q(t)}$, $t \geq 0$, where λ_0 and λ_1 need to be chosen so that (70) is satisfied and $f_{\mathbf{t}}(t)$ integrates to one. Using (61), we get

$$f_{\mathbf{s}}(s) = f_{\mathbf{t}}(g(s)) g'(s) \quad (71)$$

$$= (1 + 3\eta^2 s^2) e^{\lambda_0 + \lambda_1 s}, \quad s \geq 0. \quad (72)$$

By setting $\zeta = e^{\lambda_0}$ and $\lambda = \lambda_1$, we obtain (44).

APPENDIX II

PROOF OF THEOREM 2

Fix $\lambda \geq 0$. It follows from (16) and (17) that

$$\mathcal{C}_{\text{MNC}}(P) \leq \sup \left\{ I(\mathbf{x}; \mathbf{y}) + \lambda \left(1 - \frac{\mathbb{E}[|\mathbf{x}|^2] + P_N}{P + P_N} \right) \right\} \quad (73)$$

where the supremum is over the set of probability distributions that satisfy the power constraint (17). Next, we upper-bound the mutual information $I(\mathbf{x}; \mathbf{y})$ as

$$I(\mathbf{x}; \mathbf{y}) = h(\mathbf{y}) - h(\mathbf{y} | \mathbf{x}) \quad (74)$$

$$= h(\mathbf{y}) - h(\mathbf{n}) \quad (75)$$

$$= h(|\mathbf{y}|) + h(\underline{\mathbf{y}} | |\mathbf{y}|) + \mathbb{E}(\log |\mathbf{y}|) - h(\mathbf{n}) \quad (76)$$

$$= h(|\mathbf{y}|^2) + h(\underline{\mathbf{y}} | |\mathbf{y}|) - \log 2 - h(\mathbf{n}) \quad (77)$$

$$\leq h(|\mathbf{y}|^2) + \log(\pi) - h(\mathbf{n}) \quad (78)$$

$$= h(|\mathbf{y}|^2) - \log(eP_N) \quad (79)$$

where in (76) we used [25, Lemma 6.16] and in (77) we used [25, Lemma 6.15]. We fix now an arbitrary input pdf $f_{\mathbf{x}}(\cdot)$ that satisfies the power constraint and define the random variables $\mathbf{v} = |\mathbf{y}|^2$ and $\mathbf{w} = \mathbf{x} + j\eta|\mathbf{x}|^2\mathbf{x}$. Next, we shall obtain an upper bound on $h(\mathbf{v})$ that is valid for all $f_{\mathbf{x}}(\cdot)$. Let

$$\tilde{f}_{\mathbf{v}}(v) = \kappa e^{-\mu q(v)}, \quad v \geq 0 \quad (80)$$

for some parameters $\kappa > 0$ and $\mu > 0$. The function $q(\cdot)$ is defined in (60). We next choose κ so that $\tilde{f}_{\mathbf{v}}(v)$ is a valid pdf. To do so, we set $z = q(v)$, which implies that $g(z) = v$, and that

$$(1 + 3\eta^2 z^2) dz = dv. \quad (81)$$

Therefore, integrating $\tilde{f}(v)$ in (80), we obtain

$$\int_0^{\infty} \kappa e^{-\mu q(v)} dv = \kappa \int_0^{\infty} e^{-\mu z} (1 + 3\eta^2 z^2) dz \quad (82)$$

$$= \kappa \left(\frac{\mu^2 + 6\eta^2}{\mu^3} \right). \quad (83)$$

We see from (83) that the choice

$$\kappa = \frac{\mu^3}{\mu^2 + 6\eta^2} \quad (84)$$

makes $\tilde{f}_{\mathbf{v}}(v)$ a valid pdf. Using the definition of the relative entropy, we have

$$D(f_{\mathbf{v}}(v) \parallel \tilde{f}_{\mathbf{v}}(v)) = \int_{-\infty}^{+\infty} f_{\mathbf{v}}(v) \log\left(\frac{f_{\mathbf{v}}(v)}{\tilde{f}_{\mathbf{v}}(v)}\right) dv \quad (85)$$

$$= -h(\mathbf{v}) - \mathbb{E}[\log(\tilde{f}_{\mathbf{v}}(v))]. \quad (86)$$

Since the relative entropy is nonnegative [24, Thm. 8.6.1], we obtain

$$h(\mathbf{v}) \leq -\mathbb{E}_{\mathbf{v}}(\log(\tilde{f}_{\mathbf{v}}(\mathbf{v}))) \quad (87)$$

$$= -\log \kappa + \mu \mathbb{E}[q(\mathbf{v})] \log e. \quad (88)$$

Substituting (79) and (88) into (73), we obtain

$$\mathcal{C}_{\text{MNC}}(P) \leq -\log(eP_N) - \log \kappa + \lambda + \sup \left\{ \mu \mathbb{E}[q(\mathbf{v})] \log e - \lambda \frac{\mathbb{E}[|\mathbf{x}|^2] + P_N}{P + P_N} \right\} \quad (89)$$

$$\leq -\log(eP_N) - \log \kappa + \lambda + \max_{s>0} \left\{ \mu \mathbb{E}[q(\mathbf{v}) \mid |\mathbf{x}|^2 = s] \log e - \lambda \frac{s + P_N}{P + P_N} \right\}. \quad (90)$$

The final upper bound (21) is obtained by minimizing (90) over all $\lambda \geq 0$ and $\mu \geq 0$.

APPENDIX III

PROOF OF THEOREM 3

It follows from (88) and (79) that

$$I(\mathbf{x}; \mathbf{y}) \leq -\log(\kappa) + \mu \mathbb{E}[q(\mathbf{v})] \log e - \log(eP_N) \quad (91)$$

where $\mathbf{v} = |\mathbf{y}|^2$. Moreover,

$$\mathbb{E}[q(\mathbf{v})] = \mathbb{E}[q(|\mathbf{w} + \mathbf{n}|^2)] \quad (92)$$

$$= \mathbb{E}[q(|\mathbf{w}|^2 + |\mathbf{n}|^2 + 2\mathcal{R}(\mathbf{w}\mathbf{n}^*))]. \quad (93)$$

Next, we analyze the function $q(x)$. We have

$$q'(x) = \frac{1}{g'(q(x))} \quad (94)$$

$$= \frac{1}{1 + 3\eta^2 q^2(x)}. \quad (95)$$

Furthermore,

$$q''(x) = -\frac{6\eta^2 q(x)}{(1 + 3\eta^2 q^2(x))^3} \leq 0. \quad (96)$$

Therefore, $q(x)$ is a nonnegative concave function on $[0, \infty)$. Thus, for every real numbers $x \geq 0$ and $y \geq -x$,

$$q(x + y) \leq q(x) + q'(x)y. \quad (97)$$

Using (97) in (93), with $x = |\mathbf{w}|^2 + |\mathbf{n}|^2$ and $y = 2\mathcal{R}(\mathbf{w}\mathbf{n}^*)$, we get

$$\mathbb{E}[q(\mathbf{v})] \leq \mathbb{E}\left[q(|\mathbf{w}|^2 + |\mathbf{n}|^2) + 2q'(|\mathbf{w}|^2 + |\mathbf{n}|^2) \mathcal{R}(\mathbf{w}\mathbf{n}^*)\right]. \quad (98)$$

Using (97) once more with $x = |\mathbf{w}|^2$ and $y = |\mathbf{n}|^2$, we obtain

$$\mathbb{E}[q(\mathbf{v})] \leq \mathbb{E}\left[q(|\mathbf{w}|^2) + q'(|\mathbf{w}|^2)|\mathbf{n}|^2 + 2q'(|\mathbf{w}|^2 + |\mathbf{n}|^2) \mathcal{R}(\mathbf{w}\mathbf{n}^*)\right] \quad (99)$$

$$= \mathbb{E}\left[q(|\mathbf{w}|^2)\right] + P_N \mathbb{E}\left[q'(|\mathbf{w}|^2)\right] + 2\mathbb{E}\left[q'(|\mathbf{w}|^2 + |\mathbf{n}|^2) \mathcal{R}(\mathbf{w}\mathbf{n}^*)\right]. \quad (100)$$

We shall now bound each expectation in (100) separately. Since $|\mathbf{w}|^2 = g(|\mathbf{x}|^2)$, we have that

$$\mathbb{E}\left[q(|\mathbf{w}|^2)\right] = \mathbb{E}\left[|\mathbf{x}|^2\right] \quad (101)$$

$$\leq P \quad (102)$$

where the last inequality follows from (17). It also follows from (95) that

$$q'(|\mathbf{w}|^2) \leq 1. \quad (103)$$

Furthermore, (95) and (96) imply that the function $q'(x)$ is positive and decreasing in the interval $x \geq 0$. Therefore,

$$\mathbb{E}\left[q'(|\mathbf{w}|^2 + |\mathbf{n}|^2) \mathcal{R}(\mathbf{w}\mathbf{n}^*)\right] \leq \mathbb{E}\left[q'(|\mathbf{w}|^2 + |\mathbf{n}|^2) |\mathcal{R}(\mathbf{w}\mathbf{n}^*)|\right] \quad (104)$$

$$\leq \mathbb{E}\left[q'(|\mathbf{w}|^2) |\mathcal{R}(\mathbf{w}\mathbf{n}^*)|\right] \quad (105)$$

$$\leq \mathbb{E}\left[q'(|\mathbf{w}|^2) |\mathbf{w}| \cdot |\mathbf{n}|\right] \quad (106)$$

$$= \frac{\sqrt{\pi P_N}}{2} \mathbb{E}[q'(|\mathbf{w}|^2) |\mathbf{w}|] \quad (107)$$

$$\leq \frac{\sqrt{\pi P_N}}{2} \max_{t \geq 0} \{tq'(t^2)\} \quad (108)$$

$$= \frac{\sqrt{\pi P_N}}{2} \max_{t \geq 0} \left\{ \frac{t}{1 + 3\eta^2 q^2(t^2)} \right\} \quad (109)$$

where (107) holds because $\mathbb{E}[|\mathbf{n}|] = \sqrt{\pi P_N/4}$ and the last equality follows from (95). To calculate the maximum in (109), we use the change of variables $t^2 = x + \eta^2 x^3$ to obtain

$$\max_{t \geq 0} \left\{ \frac{t}{1 + 3\eta^2 q^2(t^2)} \right\} = \max_{x \geq 0} \left\{ \frac{\sqrt{x + \eta^2 x^3}}{1 + 3\eta^2 x^2} \right\} \quad (110)$$

$$= \frac{1}{12^{3/8} \sqrt{(\sqrt{3} - 1)} \eta} \quad (111)$$

where the last step follows by some standard algebraic manipulations that involve finding the roots of the derivative of the objective function on the RHS of (110). Substituting (111) into (109), we obtain

$$\mathbb{E}[q'(|\mathbf{w}|^2 + |\mathbf{n}|^2) \mathcal{R}(\mathbf{w}\mathbf{n}^*)] \leq \frac{\sqrt{\pi P_N}}{2 \times 12^{3/8} \sqrt{(\sqrt{3} - 1)} \eta}. \quad (112)$$

Substituting (102), (103), and (112) into (100), and the result into (91), we obtain

$$I(\mathbf{x}; \mathbf{y}) \leq -\log \kappa + \mu (\log e) \left\{ P + P_N + \frac{\sqrt{\pi P_N}}{12^{3/8} \sqrt{(\sqrt{3} - 1)} \eta} \right\} - \log(e P_N). \quad (113)$$

Finally, we obtain (21) by substituting (84) into (113). Since the upper bound (113) on mutual information holds for every input distribution that satisfies the power constraint, it is also an upper bound on capacity for every $\mu > 0$. To find the optimal μ , we need to minimize

$$\log\left(\frac{\mu^2 + 6\eta^2}{\mu^3}\right) + \mu(P + B) \log e = \log\left(\frac{\exp(\mu(P + B)) (\mu^2 + 6\eta^2)}{\mu^3}\right) \quad (114)$$

where B was defined in (24). Observe now that the function inside logarithm on the RHS of (114) goes to infinity when $\mu \rightarrow 0$ and when $\mu \rightarrow \infty$. Therefore, since this function is positive, it must have a minimum in the interval $[0, \infty)$. To find this minimum, we set its

derivative equal to zero and get (24). Note finally that since (20) has exactly one real root, which was proved in Appendix I-A, (24) also has exactly one real root.

APPENDIX IV

PROOF OF THEOREM 5

The proof uses similar steps as in [27, Sec. III-C]. We upper-bound the mutual information between the \mathbf{x} and \mathbf{y} expressed in polar coordinates as

$$I(\mathbf{x}; \mathbf{y}) = I(\mathbf{r}_0, \boldsymbol{\theta}_0; \mathbf{r}, \boldsymbol{\theta}) \quad (115)$$

$$= I(\mathbf{r}_0, \boldsymbol{\theta}_0; \mathbf{r}) + I(\mathbf{r}_0, \boldsymbol{\theta}_0; \boldsymbol{\theta} | \mathbf{r}) \quad (116)$$

$$= h(\mathbf{r}) - h(\mathbf{r} | \mathbf{r}_0, \boldsymbol{\theta}_0) + h(\boldsymbol{\theta} | \mathbf{r}) - h(\boldsymbol{\theta} | \mathbf{r}, \mathbf{r}_0, \boldsymbol{\theta}_0) \quad (117)$$

$$\leq h(\mathbf{r}^2) - \mathbb{E}[\log(\mathbf{r})] - \log 2 - h(\mathbf{r} | \mathbf{r}_0, \boldsymbol{\theta}_0) + \log(2\pi) - h(\boldsymbol{\theta} | \mathbf{r}, \mathbf{r}_0, \boldsymbol{\theta}_0). \quad (118)$$

In (118) we used [25, Eq. (317)] and that $h(\boldsymbol{\theta} | \mathbf{r}) \leq \log(2\pi)$. Let now $\tilde{f}_{\mathbf{r}^2}(\cdot)$ denote an arbitrary pdf for \mathbf{r}^2 . Following the same calculations as in (85)–(87), we obtain

$$h(\mathbf{r}^2) \leq -\mathbb{E}_{\mathbf{r}^2} [\log(\tilde{f}_{\mathbf{r}^2}(\mathbf{r}^2))]. \quad (119)$$

We shall take $\tilde{f}_{\mathbf{r}^2}(\cdot)$ to be a Gamma distribution with parameters $\alpha > 0$ and $\beta = (P + P_N)/\alpha$, i.e.,

$$\tilde{f}_{\mathbf{r}^2}(z) = \frac{z^{\alpha-1} e^{-z/\beta}}{\beta^\alpha \Gamma(\alpha)}, \quad z \geq 0. \quad (120)$$

Here, $\Gamma(\cdot)$ denotes the Gamma function. Substituting (120) into (119), we obtain

$$\mathbb{E}[\log(\tilde{f}_{\mathbf{r}^2}(\mathbf{r}^2))] \quad (121)$$

$$= 2(\alpha - 1)\mathbb{E}[\log(\mathbf{r})] - \alpha \frac{\mathbb{E}[\mathbf{r}_0^2] + P_N}{P + P_N} \log e - \alpha \log\left(\frac{P + P_N}{\alpha}\right) - \log(\Gamma(\alpha)). \quad (122)$$

It follows from (10) that the random variables \mathbf{r} and $\boldsymbol{\theta}_0$ are conditionally independent given \mathbf{r}_0 . Therefore,

$$h(\mathbf{r} | \mathbf{r}_0, \boldsymbol{\theta}_0) = h(\mathbf{r} | \mathbf{r}_0). \quad (123)$$

Next, we study the term $h(\boldsymbol{\theta} \mid \mathbf{r}, \mathbf{r}_0, \boldsymbol{\theta}_0)$ in (118). From Bayes' theorem and (10) it follows that for every $\theta' \in [0, 2\pi)$

$$f_{\boldsymbol{\theta} \mid \mathbf{r}, \mathbf{r}_0, \boldsymbol{\theta}_0}(\theta \mid r, r_0, \theta_0) = f_{\boldsymbol{\theta} \mid \mathbf{r}, \mathbf{r}_0, \boldsymbol{\theta}_0}(\theta - \theta' \mid r, r_0, \theta_0 - \theta'). \quad (124)$$

Therefore,

$$h(\boldsymbol{\theta} \mid \mathbf{r}, \mathbf{r}_0, \boldsymbol{\theta}_0) = \int_0^{2\pi} f_{\theta_0}(\theta_0) h(\boldsymbol{\theta} \mid \mathbf{r}, \mathbf{r}_0, \boldsymbol{\theta}_0 = \theta_0) d\theta_0 \quad (125)$$

$$= \int_0^{2\pi} f_{\theta_0}(\theta_0) h(\boldsymbol{\theta} - \theta_0 \mid \mathbf{r}, \mathbf{r}_0, \boldsymbol{\theta}_0 = 0) d\theta_0 \quad (126)$$

$$= \int_0^{2\pi} f_{\theta_0}(\theta_0) h(\boldsymbol{\theta} \mid \mathbf{r}_0, \boldsymbol{\theta}_0 = 0) d\theta_0 \quad (127)$$

$$= h(\boldsymbol{\theta} \mid \mathbf{r}, \mathbf{r}_0, \boldsymbol{\theta}_0 = 0). \quad (128)$$

Here, (127) follows because differential entropy is invariant to translations [24, Th. 8.6.3].

Substituting (122), (119), (123), and (128) into (118), we obtain

$$\begin{aligned} I(\mathbf{r}_0, \boldsymbol{\theta}_0; \mathbf{r}, \boldsymbol{\theta}) &\leq \alpha \log\left(\frac{P + P_N}{\alpha}\right) + \log(\Gamma(\alpha)) + \log(\pi) + \alpha \frac{\mathbb{E}[\mathbf{r}_0^2] + P_N}{P + P_N} \log e \\ &\quad + (1 - 2\alpha)\mathbb{E}[\log(\mathbf{r})] - h(\mathbf{r} \mid \mathbf{r}_0) - h(\boldsymbol{\theta} \mid \mathbf{r}, \mathbf{r}_0, \boldsymbol{\theta}_0 = 0). \end{aligned} \quad (129)$$

Fix $\lambda \geq 0$. We next upper bound \mathcal{C}_{MNC} using (129) as

$$\begin{aligned} \mathcal{C}_{\text{MNC}}(P) &\leq \sup \left\{ I(\mathbf{r}_0, \boldsymbol{\theta}_0; \mathbf{r}, \boldsymbol{\theta}) + \lambda \left(1 - \frac{\mathbb{E}[\mathbf{r}_0^2] + P_N}{P + P_N} \right) \right\} \\ &\leq \alpha \log\left(\frac{P + P_N}{\alpha}\right) + \log(\Gamma(\alpha)) + \log(\pi) + \lambda \\ &\quad + \sup \left\{ (\alpha \log e - \lambda) \frac{\mathbb{E}[\mathbf{r}_0^2] + P_N}{P + P_N} + (1 - 2\alpha)\mathbb{E}[\log(\mathbf{r})] - h(\mathbf{r} \mid \mathbf{r}_0) \right. \\ &\quad \left. - h(\boldsymbol{\theta} \mid \mathbf{r}, \mathbf{r}_0, \boldsymbol{\theta}_0 = 0) \right\} \end{aligned} \quad (131)$$

where the supremum is over the set of input probability distributions that satisfy (17). We complete the proof by noting that the supremum in (131) is less or equal to $\max_{r_0 > 0} \{g_{\lambda, \alpha}(r_0, P)\}$, where $g_{\lambda, \alpha}(r_0, P)$ is defined in (32).

REFERENCES

- [1] E. Agrell *et al.*, “Roadmap of optical communications,” *J. Opt.*, vol. 18, no. 6, May 2016, Art. no. 063002.
- [2] A. Mecozzi, “Limits to long-haul coherent transmission set by the Kerr nonlinearity and noise of the in-line amplifiers,” *J. Lightw. Technol.*, vol. 12, no. 11, pp. 1993–2000, Nov. 1994.
- [3] N. Merhav, G. Kaplan, A. Lapidoth, and S. Shamai (Shitz), “On information rates for mismatched decoders,” *IEEE Trans. Inform. Theory*, vol. 40, no. 6, pp. 1953–1967, Nov. 1994.
- [4] M. Secondini, E. Forestieri, and G. Prati, “Achievable information rate in nonlinear WDM fiber-optic systems with arbitrary modulation formats and dispersion maps,” *J. Lightw. Technol.*, vol. 31, no. 23, pp. 3839–3852, Dec. 2013.
- [5] T. Fehenberger, A. Alvarado, P. Bayvel, and N. Hanik, “On achievable rates for long-haul fiber-optic communications,” *Opt. Express*, vol. 23, no. 7, pp. 9183–9191, Apr. 2015.
- [6] G. Kramer, M. I. Yousefi, and F. R. Kschischang, “Upper bound on the capacity of a cascade of nonlinear and noisy channels,” in *IEEE Info. Theory Workshop (ITW)*, Jerusalem, Apr. 2015.
- [7] G. P. Agrawal, *Nonlinear Fiber Optics*, 4th ed. San Diego, CA: Elsevier, 2006.
- [8] E. Agrell, G. Durisi, and P. Johannisson, “Information-theory-friendly models for fiber-optic channels: A primer,” in *IEEE Info. Theory Workshop (ITW)*, Jerusalem, Apr. 2015.
- [9] K. V. Peddanarappagari and M. Brandt-Pearce, “Volterra series transfer function of single-mode fibers,” *J. Lightw. Technol.*, vol. 15, no. 12, pp. 2232–2241, Dec. 1997.
- [10] A. Mecozzi, C. B. Clausen, and M. Shtauf, “Analysis of intrachannel nonlinear effects in highly dispersed optical pulse transmission,” *IEEE Photon. Technol. Lett.*, vol. 12, no. 4, pp. 392–394, Apr. 2000.
- [11] A. Mecozzi and R.-J. Essiambre, “Nonlinear Shannon limit in pseudolinear coherent systems,” *J. Lightw. Technol.*, vol. 30, no. 12, pp. 2011–2024, Jun. 2012.
- [12] E. Agrell and M. Karlsson, “Influence of behavioral models on multiuser channel capacity,” *J. Lightw. Technol.*, vol. 33, no. 17, pp. 3507–3515, Sep. 2015.
- [13] M. H. Taghavi, G. C. Papen, and P. H. Siegel, “On the multiuser capacity of WDM in a nonlinear optical fiber: Coherent communication,” *IEEE Trans. Inform. Theory*, vol. 52, no. 11, pp. 5008–5022, Nov. 2006.
- [14] H. Ghozlan and G. Kramer, “Interference focusing for mitigating cross-phase modulation in a simplified optical fiber model,” in *Proc. IEEE Int. Symp. Inform. Theory*, Texas, Jun. 2010, pp. 2033–2037.
- [15] ———, “Interference focusing for simplified optical fiber models with dispersion,” in *Proc. IEEE Int. Symp. Inform. Theory*, Saint-Petersburg, Jul-Aug 2011, pp. 376–379.
- [16] K. S. Turitsyn, S. A. Derevyanko, I. Yurkevich, and S. K. Turitsyn, “Information capacity of optical fiber channels with zero average dispersion,” *Phys. Rev. Lett.*, vol. 91, no. 20, p. 203901, Nov. 2003.

- [17] M. I. Yousefi and F. R. Kschischang, “On the per-sample capacity of nondispersive optical fibers,” *IEEE Trans. Inform. Theory*, vol. 57, no. 11, pp. 7522–7541, Nov. 2011.
- [18] K. Kamran, G. Durisi, and E. Agrell, “A tighter upper bound on the capacity of the nondispersive optical fiber channel,” in *Proc. European Conference on Optical Communication (ECOC)(accepted)*, Gothenburg, Sep. 2017.
- [19] A. Vannucci, P. Serena, and A. Bononi, “The RP method: A new tool for the iterative solution of the nonlinear Schrödinger equation,” *J. Lightw. Technol.*, vol. 20, no. 7, pp. 1102–1112, Jul. 2002.
- [20] E. Forestieri and M. Secondini, “Solving the nonlinear Schrödinger equation,” in *Optical Communication Theory and Techniques*. New York, NY: Springer, 2005, pp. 3–11.
- [21] E. Ciaramella and E. Forestieri, “Analytical approximation of nonlinear distortions,” *IEEE Photon. Technol. Lett.*, vol. 17, no. 1, pp. 91–93, Jan. 2005.
- [22] K.-P. Ho, *Phase-Modulated Optical Communication Systems*. New York, NY: Springer, 2005.
- [23] A. E. Gamal and Y.-H. Kim, *Network Information Theory*. UK: Cambridge University Press, 2011.
- [24] T. M. Cover and J. A. Thomas, *Elements of Information Theory*, 2nd ed. Hoboken, NJ: Wiley, 2006.
- [25] A. Lapidoth and S. M. Moser, “Capacity bounds via duality with applications to multiple-antenna systems on flat-fading channels,” *IEEE Trans. Inform. Theory*, vol. 49, no. 10, pp. 2426–2467, Oct. 2003.
- [26] A. Papoulis and S. U. Pillai, *Probability, Random Variables, and Stochastic Processes*, 4th ed. New York, NY: McGraw-Hill Education, 2002.
- [27] G. Durisi, “On the capacity of the block-memoryless phase-noise channel,” *IEEE Commun. Lett.*, vol. 16, no. 8, pp. 1157–1160, Aug. 2012.